PARAMETRIC OPTIMIZATION OF CLOSED-LOOP SLEW CONTROL USING INTERPOLATION POLYNOMIALS

Sergei Tanygin[*]

Missions of many civilian, commercial and military satellites include slewing between multiple targeting opportunities. While the boundary conditions for the slew are set by the targets, the shape of the slew trajectory can be optimized to meet various performance metrics, such as minimizing integral of the magnitude of the angular acceleration or of the external torque. This paper investigates design and parametric optimization of the slew trajectory using blending of two simple spins. The resulting trajectory that becomes a Hermite interpolant in unit quaternion space is controlled by the blending function. Various types of blending functions permit various optimization techniques.

INTRODUCTION

Attitude trajectory optimization has been studied extensively.[1-7] In general, even seemingly simple problems such as minimum-time rest-to-rest reorientation of a rigid spacecraft subject to control limits have eluded a closed-form solution.[1-4] Proposed numerical solutions to this and other attitude trajectory optimization problems include various combinations of direct and indirect optimization methods, all of which tend to be computationally expensive.[1-7] This paper describes a method for generating a smooth slew trajectory with known boundary points via blending of two simple spins. The shape of the slew trajectory is controlled by a scalar blending function, which in turn can adopt various parameterizations. Thus, a full trajectory optimization can be replaced by a parametric optimization carried out on a simpler and more structured formulation. While results of the parametric optimization may not be as optimal as those of the full trajectory optimization, computational advantages of the former make it suitable for near-real time slew design.

---

[*] Member AAS and AIAA. Sr. Astrodynamics Specialist, Analytical Graphics, Inc., 220 Valley Creek Blvd., Exton, PA 19341, stanygin@agi.com

TRANSITION BETWEEN TRAJECTORIES USING BLENDING

A basic concept of blending is quite straightforward and can be applied to various types of trajectories. In general, it simply means that a new trajectory is a weighted combination or a blend of the two known trajectories which are typically designed to satisfy certain boundary conditions. As mentioned in the introduction, this partitioning of the trajectory suggests alternative approaches to its optimization. For example, an efficient optimization of the blending function may prove to be a reasonable proxy to a full trajectory optimization that often results in computationally expensive problems unsolvable in a closed form. A specific type of blending discussed in this paper produces a particularly simple C^1 Hermite interpolant that permits many straightforward parameterizations.[8,9] Such characteristics are important for generating physically realizable trajectories along which optimization metrics can be integrated in a closed form. This type of blending includes a constant rate extrapolation of the departure trajectory from the blending start time into the future and a constant rate extrapolation of the arrival trajectory from the blending end time into the past (Fig.1). The actual blending occurs by combining the two extrapolated trajectories via a scalar blending function which varies from 0 at the departure time to 1 at the arrival time and which departs and arrives with 0 rate of change (Fig.2). At any time between the departure and arrival, the blended trajectory is a weighted combination of the two extrapolated trajectories where the blending function value indicates the proportion of the extrapolated arrival trajectory in the blend (Fig.1). A manner in which trajectories are combined depends on the space in which they are defined. For example, a simple weighted sum combines trajectories in Euclidean space $\Re^n$. However, for attitude trajectories a more complicated blending scheme is required: the one that relies on a mapping between the Euclidean space $\Re^3$ and the unit quaternion space S^3.
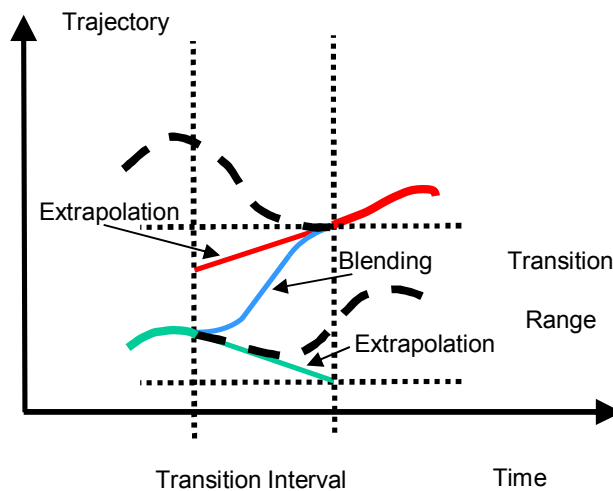
Figure 1 Transition by blending constant rate extrapolated trajectories
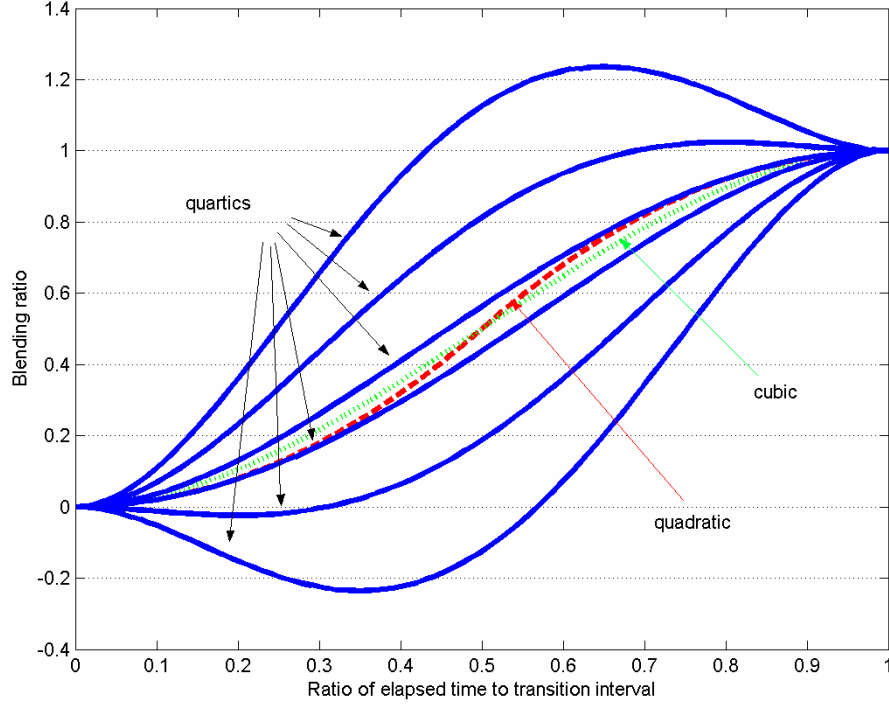
Figure 2 Examples of blending functions

LOGARITHMIC AND EXPONENTIAL MAPS

Majority of interpolants, splines and blending functions are originally developed in Euclidean space $\Re^n$, i.e. their useful properties rely on the existence of Euclidean metric. A common approach for applying them to trajectories that reside in non-Euclidean spaces includes mapping trajectories to and from some related Euclidean space in which standard interpolants, splines and blending functions can operate natively.[9-13] Since the non-Euclidean space $SO(3)$ which contains attitude matrices has many geometric properties which are much different from those of the Eucledian space $\Re^3$, it is advantageous to employ unit quaternions instead. They reside on the 3-sphere S^3 embedded in $\Re^4$, have the same local geometry as attitude matrices in $SO(3)$ and possess simple mappings to and from the Euclidean space $\Re^3$. A unit quaternion can be defined by four coordinates, three vector part coordinates and one scalar part coordinate, all related via the unit norm constraint.[14] At any point on the 3-sphere, i.e. for any unit quaternion, there exists a tangential space defined as a 3-plane. The plane contains all vectors in $\Re^4$ that are orthogonal to the associated unit quaternion. The plane orthogonal to the identity unit quaternion is particularly useful. Since this quaternion has zero vector part, any and all pure quaternions, i.e. quaternions that have zero scalar part, belong to its

tangent space. Geometry of pure quaternions is equivalent to Euclidean geometry of vectors in $\Re^3$. In other words, the Euclidean space $\Re^3$ is a tangential space for the identity unit quaternion in S^3, $T_1 S^3 \equiv \Re^3$ (Fig. 3). The mappings between the two spaces can be explained using Taylor series expansion of the exponential operator applied to a pure quaternion (i.e. applied to a vector in $\Re^3$). This exponential map, $\exp : R^3 \rightarrow S^3$, as well as its inverse, $\log : S^3 \rightarrow R^3$, the logarithmic map, are presented below (Fig.3):[†][12,13]

$$\exp\{\mathbf{r}\} = \begin{cases} (\dfrac{\sin\|\mathbf{r}\|}{\|\mathbf{r}\|}\mathbf{r}, \cos\|\mathbf{r}\|), & \|\mathbf{r}\| > 0 \\ (\mathbf{r},1), & \|\mathbf{r}\| = 0 \end{cases} , \tag{1}$$

$$\log\{q\} = \log\{\mathbf{q_v}, q_s\} = \frac{\arccos q_s}{\sqrt{1-q_s^2}} \mathbf{q_v} . \tag{2}$$
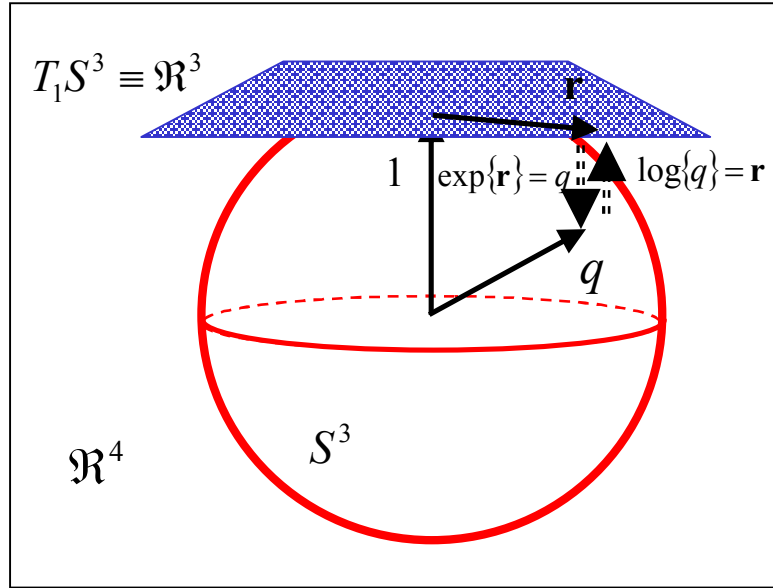
Figure 3 Logarithmic and exponential mapping between S^3 and $\Re^3$

Before completing discussion about unit quaternion tangent spaces, it is instructive to evaluate derivative of a unit quaternion and its relationship to the angular velocity of rotation. The derivative $\dot{q}$ is inherently orthogonal to the unit quaternion $q \in S^3$ and of course lies in its tangent space, $\dot{q} \in T_q S^3 \subset \Re^4$ (Fig.4). The derivative is a quaternion, but not necessarily a unit quaternion. A key transformation occurs when the coordinates are changed in a manner that makes the quaternion in question the identity.

[†] Note that, except for the constant scaling factor of 2 related to the metric change between S^3 and $SO(3)$, these maps are equivalent to relationships between quaternion and rotation vector representations of attitude.

The transformation is accomplished by multiplying the quaternion it by its conjugate $\bar{q}$: $1 = q \otimes \bar{q}$. With this change of coordinates, the tangent plane and the derivative vector in it are rotated into: $\dot{q} \otimes \bar{q} \in T_1 S^3 \equiv \mathfrak{R}^3$. Note that the transformed derivative vector is a pure quaternion (or a simple vector in $\mathfrak{R}^3$) and that it is exactly one half of the angular velocity of rotation represented by the quaternion q . The difference in size reflects the difference in metrics between S^3 and $SO(3)$ due to their 2-to-1 relationship (Fig.4).
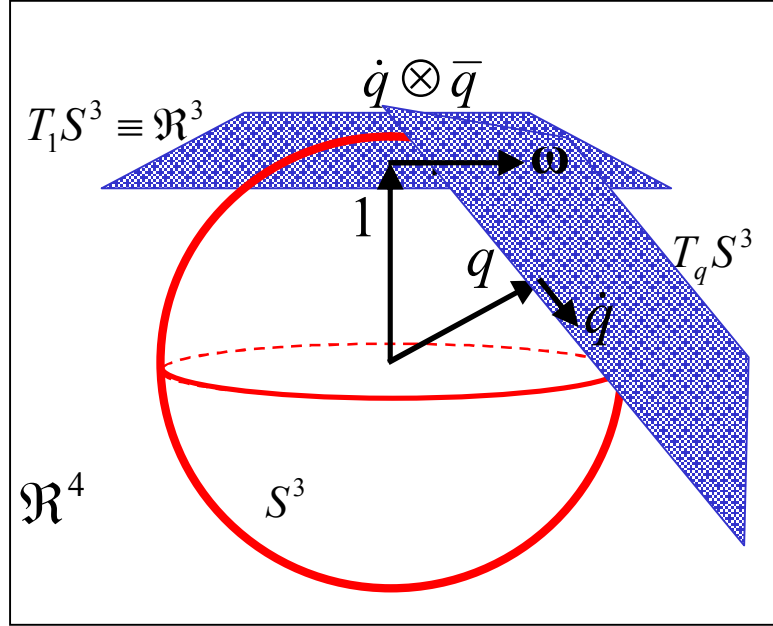
Figure 4 Quaternion and angular velocity relationship

BLENDING OF SPINS

Provided with the logarithmic and exponential maps to and from the Euclidean space $\mathfrak{R}^3$, interpolation, splining and blending of unit quaternion trajectories can proceed. A specific blending type evaluated in this paper requires that departure and arrival trajectories be extrapolated with constant rate of change. Simplicity of this requirement is one of the main advantages of applying this type of blending to attitude problems. Indeed, a constant rate of change extrapolation of attitude trajectory is readily available: it is just a constant angular velocity spin.[12] This simplicity translates into an equally straightforward formulation for the spins in unit quaternion space: the departure and arrival unit quaternion curves are[12,13]

$$C_1(t,t_1,q_1,\boldsymbol{\omega}_1) = \cos\left[\frac{\|\boldsymbol{\omega}_1\|}{2}(t-t_1)\right]q_1 + \frac{2}{\|\boldsymbol{\omega}_1\|}\sin\left[\frac{\|\boldsymbol{\omega}_1\|}{2}(t-t_1)\right]\dot{q}_1, \qquad (3)$$

and

$$C_2(t,t_2,q_2,\boldsymbol{\omega_2}) = \cos\left[\frac{\|\boldsymbol{\omega_2}\|}{2}(t-t_2)\right]q_2 + \frac{2}{\|\boldsymbol{\omega_2}\|}\sin\left[\frac{\|\boldsymbol{\omega_2}\|}{2}(t-t_2)\right]\dot{q}_2, \qquad (4)$$

respectively, where quaternion derivatives are computed using known angular velocities:[12-14]

$$\dot{q}_1 = \frac{1}{2}\boldsymbol{\omega}_1 \otimes q_1, \qquad (5)$$

$$\dot{q}_2 = \frac{1}{2}\boldsymbol{\omega_2} \otimes q_2, \qquad (6)$$

where subscript 1 indicates departure and subscript 2 indicates arrival. Note that these quaternion curves that represent constant angular velocity spins are great arcs on the 3-sphere and that they depend on time t only explicitly, i.e. all other parameters in their formulation are considered to be known constants. Given these curves at any time between the departure and arrival, the relative closeness of the blended quaternion to the departure curve is determined by the value of the blending function at that time. In order to define the blended quaternion, the direct path from a point on the departure spin to a point on the arrival spin must be evaluated at that time as well. Of course, the direct path on the 3-sphere is also a great arc, but in this case it is defined between synchronous points on the two curves: $\left(C_2 \otimes \overline{C}_1\right) \in S^3$. As discussed earlier, the blending should occur in the Euclidean space $\Re^3$, transformation to which is accomplished via the logarithmic map: $\log\left\{C_2 \otimes \overline{C}_1\right\} \in \Re^3$. Once in $\Re^3$, the distance along the path is scaled according to the blending function f and the resulting path is transformed back to S^3 using the exponential map: $\exp\left\{f \log\left\{C_2 \otimes \overline{C}_1\right\}\right\} \in S^3$, (Fig.5). A final transformation moves the blended quaternion from being relative to the departure curve to being relative to the original reference in which all trajectories are defined:[12-13]

$$q(t,t_1,t_2,q_1,\boldsymbol{\omega_1},q_2,\boldsymbol{\omega_2},f) = \exp\left\{f \log\left\{C_2 \otimes \overline{C}_1\right\}\right\} \otimes C_1. \qquad (7)$$

If the blending function $f(t,t_1,t_2) \in C^1$ satisfies the following boundary conditions:

$$f(t_1,t_1,t_2) = 0, \ f(t_2,t_1,t_2) = 1, \ \dot{f}(t_1,t_1,t_2) = 0, \ \dot{f}(t_2,t_1,t_2) = 0 \qquad (8)$$

the blended quaternion curve represents a smooth slew that satisfies both attitude and angular velocity boundary conditions:

$$q(t_1) = q_1, \ q(t_2) = q_2, \ \boldsymbol{\omega}(t_1) = \boldsymbol{\omega_1}, \ \boldsymbol{\omega}(t_2) = \boldsymbol{\omega_2}. \qquad (9)$$

Closed form expressions for angular velocity and angular acceleration can be obtained via straightforward differentiation of the quaternion curve as shown in the Appendix (Eqs.(44,52)). These rigorous expressions contain trigonometric and inverse trigonometric functions, which coupled with various types of blending functions, are likely to present a challenge for computing integrals for many optimization metrics. Therefore, although the blended quaternion curve is rigorously described in the closed form, it is desirable to look for approximations that facilitate computation of integrals along the curve.
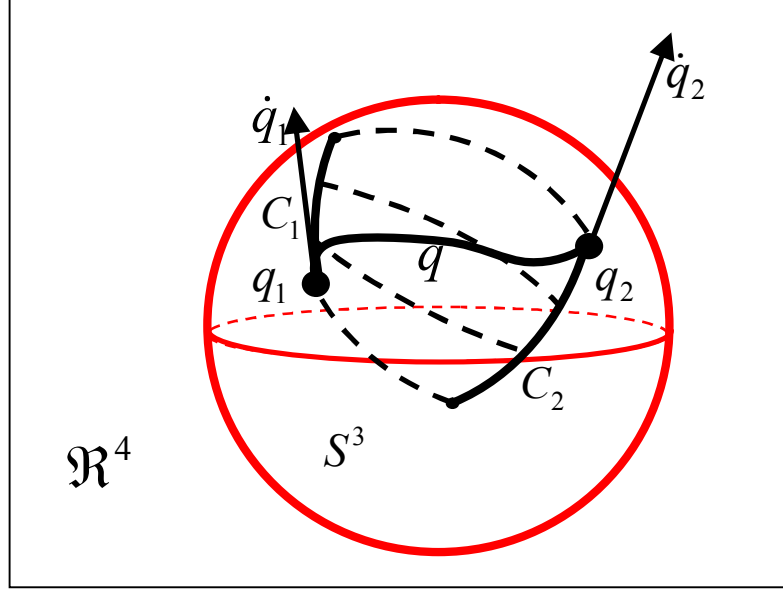
Figure 5 Blending of spins

LINEARIZED BLENDING OF SPINS IN QUATERNION SPACE

The presence of trigonometric functions in quaternion curve formulations is a natural byproduct of being located on the 3-sphere. The blended curve formulation presented in this paper combines three great arc curves: two great arcs representing extrapolated spins and a third great arc that at any time during the blending connects synchronous points on the two spin arcs (Fig.5). A natural first order approximation in this case relies on limiting of all three great arcs to a small region of the 3-sphere, where planar formulations in $\Re^4$ can replace spherical formulations in S^3. In other words, it limits the transition range (Fig.1) to a small region of the 3-sphere. Note that 2-to-1 relationship between S^3 and $SO(3)$ is advantageous in this case, because the limiting arc length on the 3-sphere is doubled when converted to a limiting eigen-angle displacement in $SO(3)$. Linearization of the extrapolated spins yields:

$$C_1(t,t_1,q_1,\boldsymbol{\omega_1}) \approx \widetilde{C}_1(t,t_1,q_1,\boldsymbol{\omega_1}) = q_1 + (t-t_1)\dot{q}_1, \tag{10}$$

$$C_2(t,t_2,q_2,\boldsymbol{\omega_2}) \approx \tilde{C}_2(t,t_2,q_2,\boldsymbol{\omega_2}) = q_2 + (t-t_2)\dot{q}_2 . \tag{11}$$

A linearized blend of these approximate curves produces a desired approximation for the blended curve:

$$q(t,t_1,t_2,q_1,\boldsymbol{\omega_1},q_2,\boldsymbol{\omega_2},f) \approx \tilde{q}(t,t_1,t_2,q_1,\boldsymbol{\omega_1},q_2,\boldsymbol{\omega_2},f) = \tilde{C}_1 + f\left[\tilde{C}_2 - \tilde{C}_1\right]. \tag{12}$$

Note that these approximations take quaternion curves off the 3-sphere, so they are no longer unit quaternion curves in S^3 and, thus, do not represent actual attitude motions (Fig. 6). However, the approximations are still adequate for a less stringent task of capturing representative integral metrics for optimization. Closed form approximations for angular velocity and angular acceleration are obtained in a manner similar to that used for rigorous expressions, except that quaternion derivatives are evaluated along the linearized blended curve. The resulting approximate expressions permit the following useful partitioning:

$$\boldsymbol{\omega}(t,t_1,t_2,q_1,\boldsymbol{\omega_1},q_2,\boldsymbol{\omega_2},f) \approx \tilde{\boldsymbol{\omega}}(t,t_1,t_2,q_1,\boldsymbol{\omega_1},q_2,\boldsymbol{\omega_2},f) = \mathbf{QF}, \tag{13}$$

$$\dot{\boldsymbol{\omega}}(t,t_1,t_2,q_1,\boldsymbol{\omega_1},q_2,\boldsymbol{\omega_2},f) \approx \tilde{\dot{\boldsymbol{\omega}}}(t,t_1,t_2,q_1,\boldsymbol{\omega_1},q_2,\boldsymbol{\omega_2},f) = \mathbf{Q\dot{F}}, \tag{14}$$

where $\mathbf{Q}(q_1,\boldsymbol{\omega_1},q_2,\boldsymbol{\omega_2}) = \begin{bmatrix} \mathbf{Q_1} & \mathbf{Q_2} & \mathbf{Q_3} & \mathbf{Q_4} & \mathbf{Q_5} & \mathbf{Q_6} \end{bmatrix} \in \mathfrak{R}^{3\times6}$ serves a set of 6 basis vectors, $\mathbf{Q_i}(q_1,\boldsymbol{\omega_1},q_2,\boldsymbol{\omega_2}) \in \mathfrak{R}^3$, which are only functions of the boundary conditions and do not depend on the time or the blending function; and where $\mathbf{F}(f,t,t_1,t_2) \in \mathfrak{R}^6$ contains a vector of 6 coordinates for the basis, $F_i(f,t,t_1,t_2) \in \mathfrak{R}$, that are independent from the boundary conditions and only depend on the time and the blending function (Eqs.(53-72)). This partitioning offers a better structured approach to computing integral metrics.
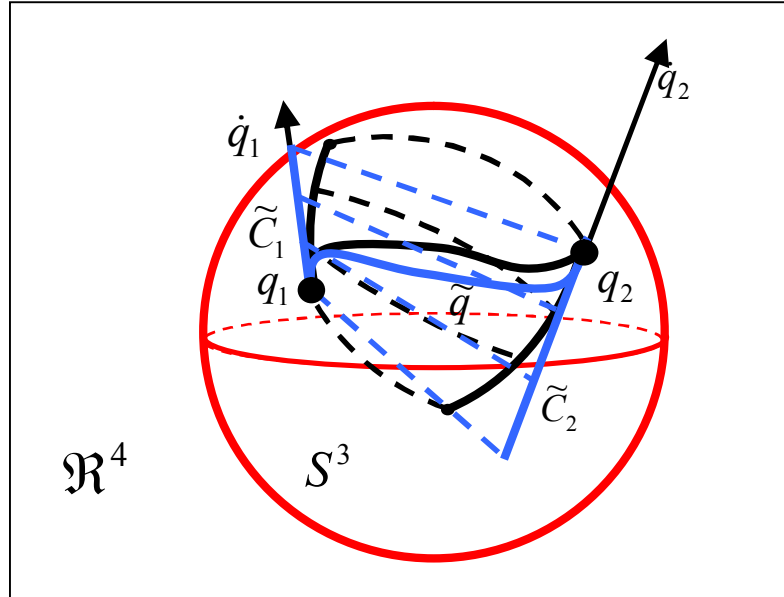
Figure 6 Linearized blending of spins

PERFORMANCE METRICS FOR PARAMETRIC OPTIMIZATION

Various performance metrics include angular velocity and angular acceleration.[6] Arguably the simplest one among them integrates magnitude of the angular acceleration. The alternative metric derived from the approximate angular acceleration becomes:

$$\widetilde{I}_{\dot{\omega}}(t_1, t_2, q_1, \boldsymbol{\omega_1}, q_2, \boldsymbol{\omega_2}, f) = \frac{1}{2} \int_{t_1}^{t_2} \left\| \widetilde{\dot{\boldsymbol{\omega}}} \right\|^2 dt = \frac{1}{2} \sum_{i=1}^{6} \sum_{j=1}^{6} W_{ij} \Phi_{ij} , \tag{15}$$

where

$$W_{ij}(q_1, \boldsymbol{\omega_1}, q_2, \boldsymbol{\omega_2}) = W_{ji}(q_1, \boldsymbol{\omega_1}, q_2, \boldsymbol{\omega_2}) = \mathbf{Q_i^T Q_j} \in \Re \tag{16}$$

and

$$\Phi_{ij}(f, t_1, t_2) = \Phi_{ji}(f, t_1, t_2) = \int_{t_1}^{t_2} \dot{F}_i \dot{F}_j dt \in \Re . \tag{17}$$

As parametric optimization requires[5-7] various partial derivatives can be readily computed form this formulation. For example, since any variation in boundary conditions only affects some basis vectors, $\mathbf{Q_k}$ and none of the basis coordinates F_i, the following partial derivative can be computed:

$$\frac{\partial}{\partial \mathbf{Q_k}} \widetilde{I}_{\dot{\omega}} = \sum_{i=1}^{6} \mathbf{Q_i^T} \Phi_{ik} . \tag{18}$$

Conversely, any variation in parameters $\mathbf{p}$ of the blending function only affects the basis coordinates and none of the basis vectors:

$$\frac{\partial}{\partial \mathbf{p}} \widetilde{I}_{\dot{\omega}} = \frac{1}{2} \sum_{i=1}^{6} \sum_{j=1}^{6} W_{ij} \frac{\partial}{\partial \mathbf{p}} \Phi_{ij} . \tag{19}$$

A more complex performance metric integrates magnitude of the external torque applied to the rigid body.[6,14] Approximation of the torque based on the approximate angular velocity and acceleration yields:

$$\widetilde{\mathbf{M}}(t, t_1, t_2, q_1, \boldsymbol{\omega_1}, q_2, \boldsymbol{\omega_2}, f) = \mathbf{IQ\dot{F}} + (\mathbf{QF}) \times (\mathbf{IQF}), \tag{20}$$

where $0 < \mathbf{I} = \mathbf{I^T} \in \Re^{3 \times 3}$ is the rigid-body inertia matrix. Although more complicated than the angular acceleration, this expression too can be used in the alternative performance metric:

$$I_M(t_1, t_2, q_1, \boldsymbol{\omega_1}, q_2, \boldsymbol{\omega_2}, f) = \frac{1}{2} \int_{t_1}^{t_2} \left\| \tilde{\mathbf{M}} \right\|^2 dt . \tag{21}$$

Note that, while these approximate formulations are simpler than their rigorous counterparts, a determining factor in easing solutions to the parametric optimization remains the type of the blending function: it determines the ease or difficulty of computing the integrals and partial derivatives. Therefore, it is instructive to consider several examples of blending functions.

EXAMPLES

One of the most straightforward types of the blending function that satisfies the boundary conditions (Eq.(8)) are various degree polynomials of t. For example, it is possible to create a continuous and smooth blending function by piecing together two quadratic polynomials:[12,13]

$$f_{II}(t, t_1, t_2) = \begin{cases} \dfrac{2(t-t_1)^2}{T^2}, & t_1 \le t \le \dfrac{t_1 + t_2}{2} \\ -\dfrac{2(t-t_1)^2}{T^2} + \dfrac{4(t-t_1)}{T} - 1, & \dfrac{t_1 + t_2}{2} < t \le t_2 \end{cases} , \tag{22}$$

or a single cubic polynomial:

$$f_{III}(t, t_1, t_2) = -\frac{2(t-t_1)^3}{T^3} + \frac{3(t-t_1)^2}{T^2} . \tag{23}$$

Higher degree polynomials can satisfy the boundary conditions and have one or more free parameters. For example, the following blending function constructed using a quartic polynomial has one free parameter p, the quartic coefficient:

$$f_{IV}(t, t_1, t_2, p) = \frac{(t-t_1)^2 [3t_2 - t_1 - 2t]}{T^3} + p(t-t_1)^2 (t-t_2)^2 . \tag{24}$$

This means that there is in fact an entire family of quartic blending functions parameterized by the quartic coefficient. This also means that parametric optimization can be carried out with respect to this coefficient. What is more, for a simple metric, such as the integrated magnitude of the angular acceleration, the optimal value of the quartic coefficient ends up being one of the roots of the cubic polynomial in p:

$$\frac{\partial}{\partial p} \tilde{I}_{\dot{\omega}}(t_1, t_2, q_1, \boldsymbol{\omega_1}, q_2, \boldsymbol{\omega_2}, f_{IV}) = a_0 + a_1 p + a_2 p^2 + a_3 p^3 = 0 , \tag{25}$$

where polynomial coefficients $a_i(t_1, t_2, q_1, \omega_1, q_2, \omega_2)$ shown in Appendix are functions of the boundary conditions (Eqs.(73-76)).

Consider a numerical example in which a slew is designed to achieve a net 40 deg rotation about the x-axis in 1 second, given the following boundary angular velocities:

$$\omega_1 = \begin{bmatrix} 0.1 & 0.2 & 0.3 \end{bmatrix}^T rad/s, \ \omega_2 = \begin{bmatrix} -0.3 & 0.2 & 0.1 \end{bmatrix}^T rad/s \qquad (26)$$

Resulting angular velocity components computed with the cubic blending function using both exact and approximate formulations show satisfactory agreement (Figs. 7, 8) as do angular acceleration components, which are quite high (Figs. 9, 10). Evolution of the eigen-angle relative to the initial orientation shows that the angle reaches the intended value as prescribed (Fig. 11). Evolution of another eigen-angle, which is measured between the two extrapolated spins, shows that satisfactory approximation is achieved even when transition range spans almost 60 deg (Fig. 12). The remaining examples compare performances of the quadratic, cubic and quartic blending functions. The integrated magnitude of the angular acceleration is evaluated for each of these functions. For the quartic blending function, the metric is evaluated as a function of the quartic parameter (Figs. 13, 14). The cubic function performs significantly better then the quadratic function. However, the optimal value of the quartic parameter makes the quartic function perform even better. Note that optimal value computed analytically as a root of the cubic polynomial in p (Eq. 25) is in an excellent agreement with the sampled data (Fig. 14). Finally, the integrand of the metric, the magnitude of the angular acceleration is shown to demonstrate the differences of its evolutions with different blending functions (Fig. 15).

CONCLUSIONS

The paper demonstrated how a closed-form slew trajectory designed via blending of two simple spins can be linearized and used for defining closed-form performance metrics. Linearization leads to partitioning of the slew trajectory into a linear combination of 6 constant basis vectors and 6 time dependent basis coordinates. This representation eases formulation, computation and optimization of various integral metrics. Examples demonstrate viability of the linearization and optimization even for moderately large angle slews.
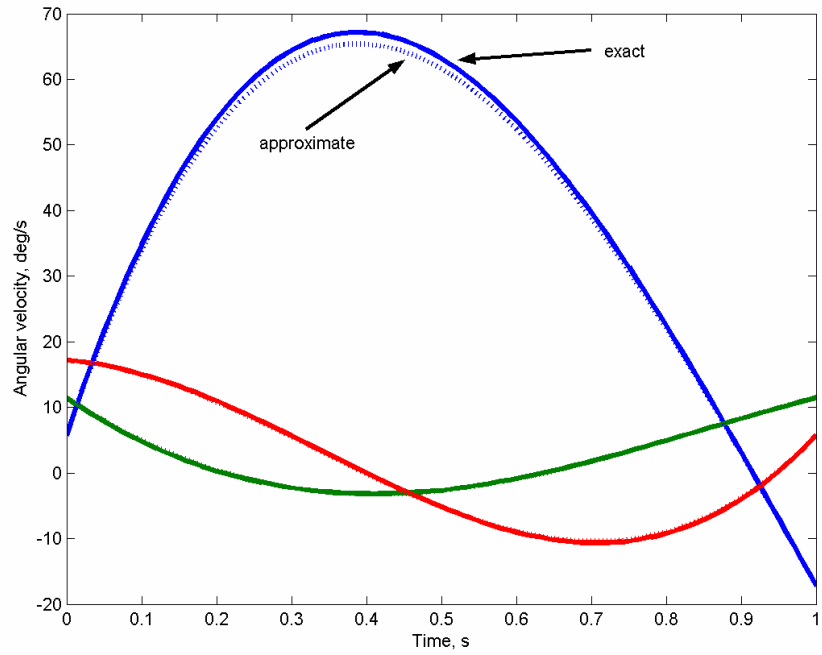
Figure 7 Angular velocity components using cubic blending
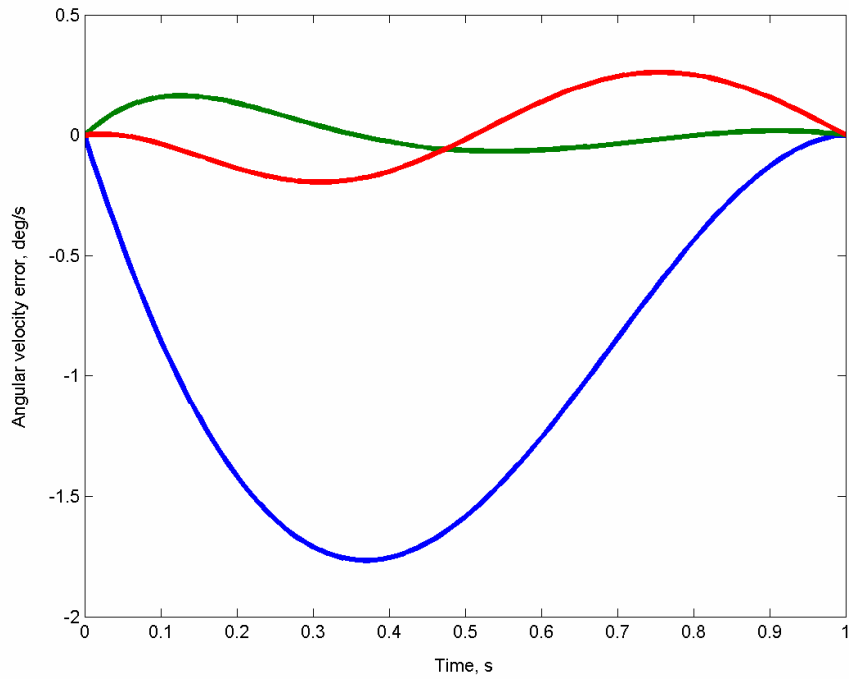
Figure 8 Approximation errors in angular velocity components using cubic blending
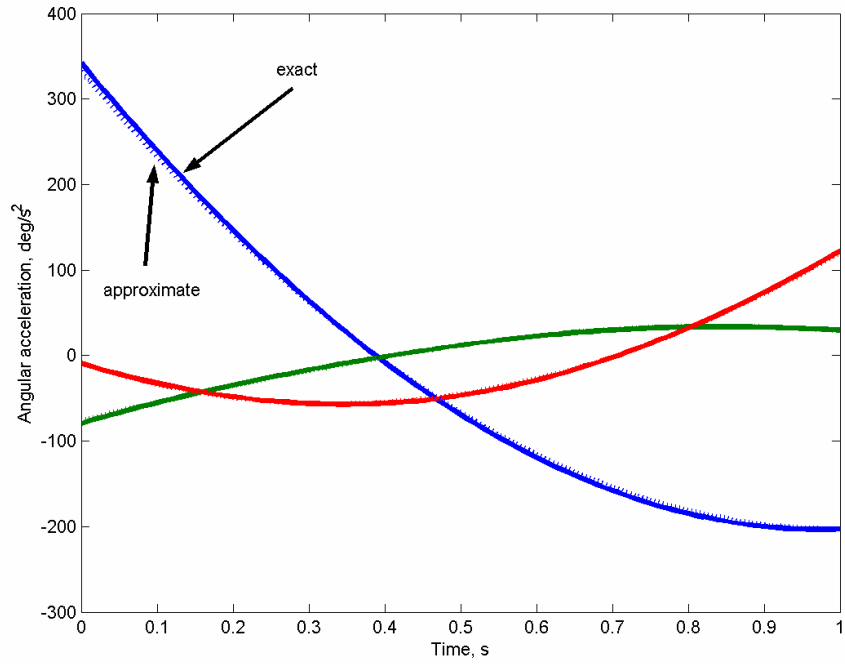
Figure 9 Angular acceleration components using cubic blending
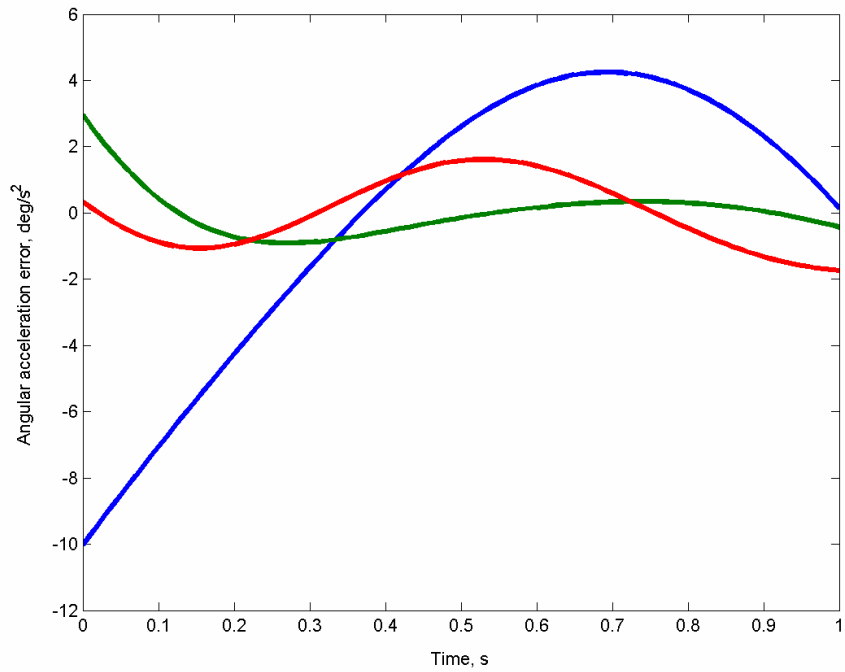
Figure 10 Approximation errors in angular acceleration components using cubic blending
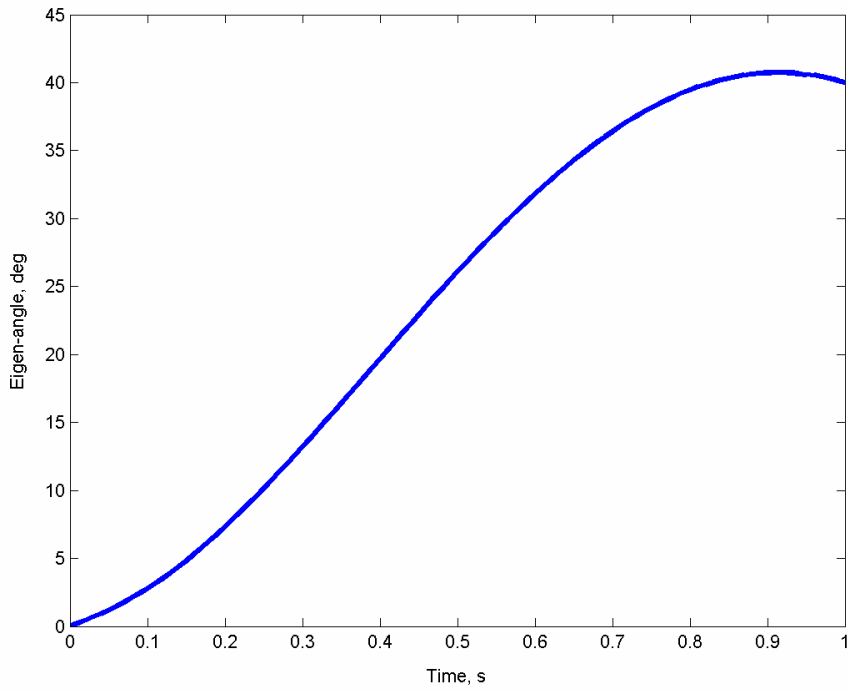
Figure 11 Eigen-angle relative to initial orientation using cubic blending
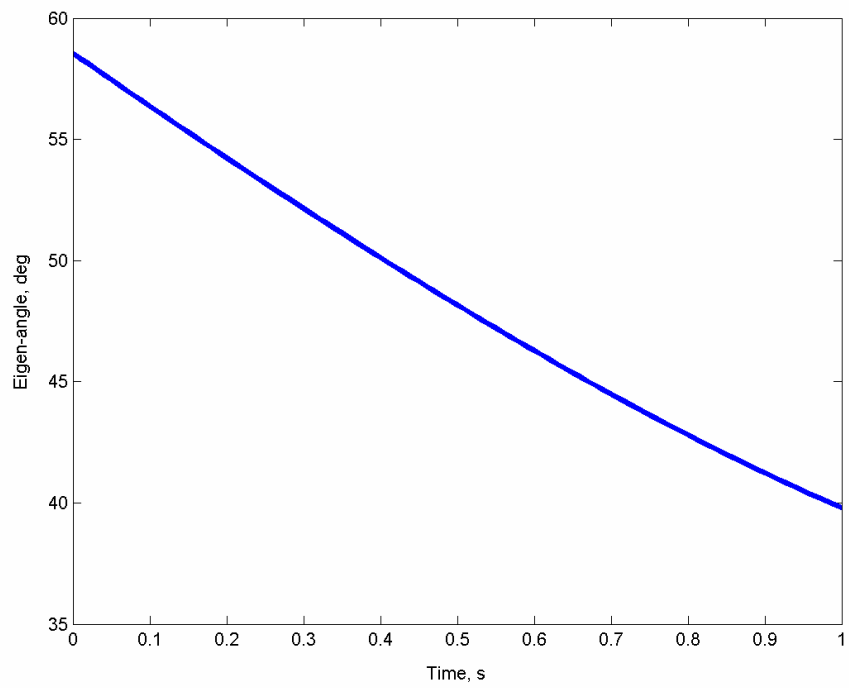
Figure 12 Eigen-angle between departure and arrival spins using cubic blending
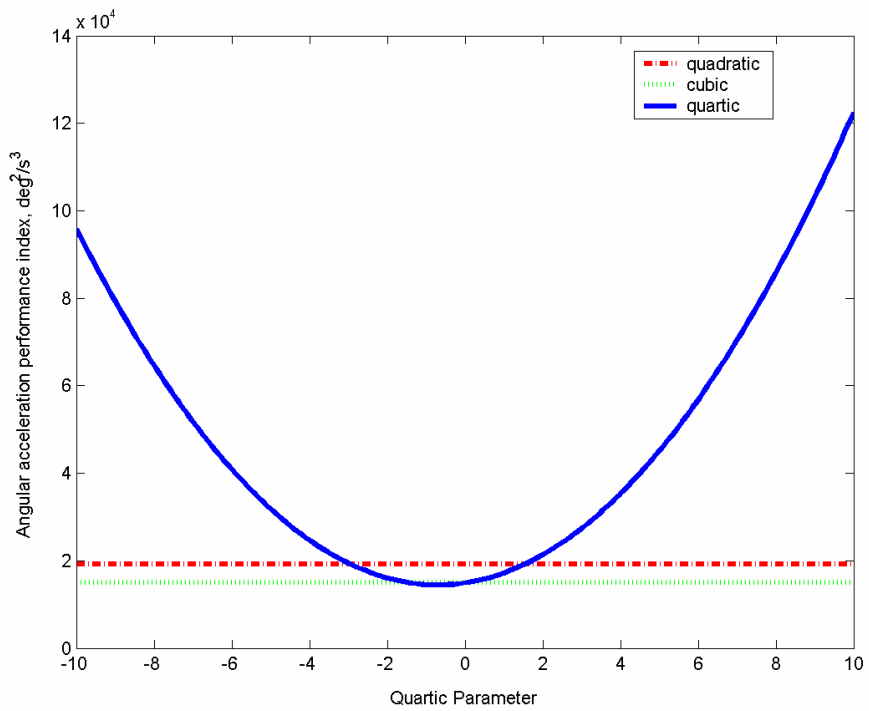
Figure 13 Angular acceleration performance metric with various blending
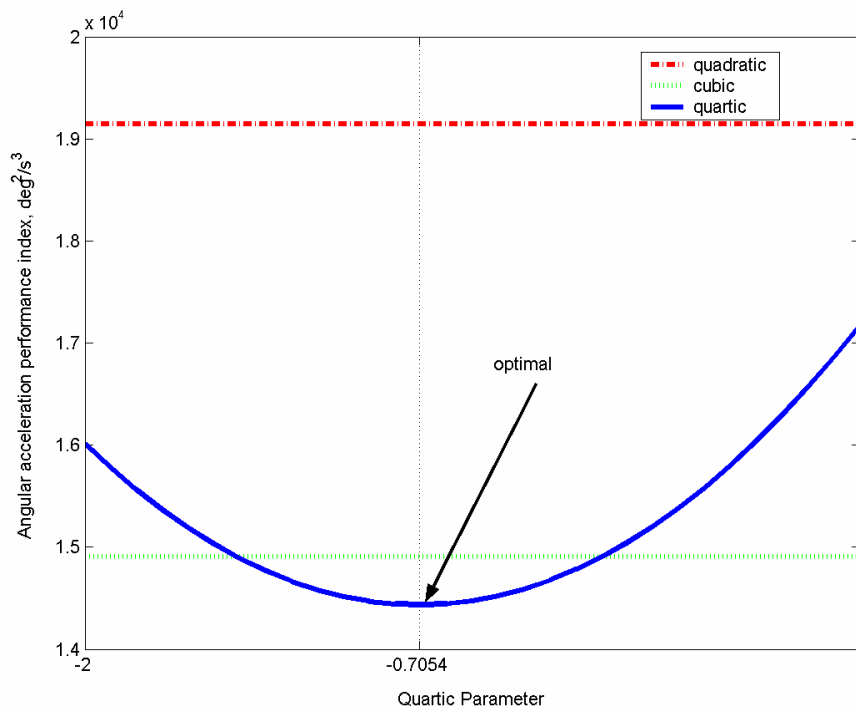
Figure 14 Details of parametric optimization with quartic blending
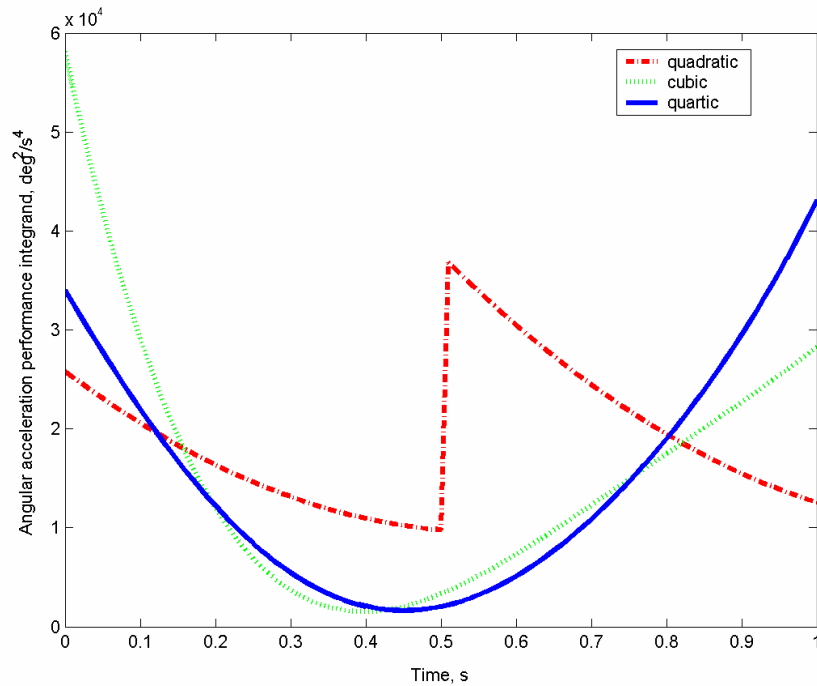
Figure 15 Integrand of angular acceleration performance metric including optimal quartic blending

REFERENCES

1. R.J. Proulx and I.M. Ross, "Time-Optimal Reorientation of Asymmetric Rigid Bodies," Paper AAS 01-384, AAS/AIAA Astrodynamics Specialists Conference, Quebec City, Quebec, Canada, July-Aug, 2001.

2. S.L. Scrivener and R.C. Thompson, "Survey of Time-Optimal Attitude Maneuvers," *Journal of Guidance, Control and Dynamics*, Vol.17, No.2, 1994, pp.225-233.

3. K.D. Bilimoria and B. Wie, "Time-Optimal Three-Axis Reorientation of a Rigid Spacecraft, "*Journal of Guidance, Control and Dynamics*, Vol.16, No.3, 1993, pp.446-452.

4. F. Li and P.M. Bainum, "Numerical Approach for Solving Rigid Spacecraft Minimum-Time Attitude Maneuvers," *Journal of Guidance, Control and Dynamics*, Vol.13, No.1, 1990, pp.38-45.

5. R. F. Stengel, *Optimal Control and Estimation,* Dover Publications Inc., New York, 1994.

6. B. Wie, *Space Vehicle Dynamics and Control,* AIAA Education Series, Reston VA, 1998.

7. D. A. Pierre, *Optimization Theory with Applications,* Dover Publications Inc., New York, 1986.

8. S. Tanygin, "Attitude Interpolation," Paper AAS 03-197, AAS/AIAA Space Flight Mechanics Meeting, Ponce, Puerto-Rico, Feb. 2003.

9. P.J. Davis, *Interpolation and Approximation*, Dover Publications Inc., New York, 1975.

10. K. Shoemake, "Animation Rotation with Quaternion Curves," *Computer Graphics,* Vol.19(3), 1985, pp. 245-254.

11. A.H. Barr, B. Currin, S. Gabriel, and J.F. Hughes, "Smooth Interpolation of Orientations with Angular Velocity Constraints using Quaternions," *SIGGRAPH' 92* Proceedings, 1992, pp. 313-320.

12. K-W. Nam and M-S. Kim, "Hermite Interpolation of Solid Orientations Based on a Smooth Blending of Two Great Circular Arcs on SO(3)," *in Computer Graphics: Development in Virtual Environments,* Academic Press, 1995, pp. 171-183.

13. S. Tanygin and J. Woodburn "Optimal Switching Between Targets Using Rate-Limited Slews," Paper AAS 05-331, AAS/AIAA Astrodynamics Specialists Conference, Lake Tahoe, CA, Aug. 2005.

14. M.D. Shuster, "A Survey of Attitude Representations," *Journal of the Astronautical Sciences*, Vol.41, No.4, 1993, pp.439-517.

APPENDIX

A detailed formulation for the blended slew in terms of quaternions is presented below along with some helpful intermediate variables:

$$D(t, t_1, t_2, q_1, \boldsymbol{\omega_1}, q_2, \boldsymbol{\omega_2}) = C_2 \otimes \overline{C}_1 \in S^3, \tag{27}$$

$$D_s(t, t_1, t_2, q_1, \boldsymbol{\omega_1}, q_2, \boldsymbol{\omega_2}) = scalar\ part\{D\} \in R, \tag{28}$$

$$\mathbf{D_v}(t, t_1, t_2, q_1, \boldsymbol{\omega_1}, q_2, \boldsymbol{\omega_2}) = vector\ part\{D\} \in R^3, \tag{29}$$

$$D_v(t, t_1, t_2, q_1, \boldsymbol{\omega_1}, q_2, \boldsymbol{\omega_2}) = \|\mathbf{D_v}\| = \sqrt{1 - D_s^2}, \tag{30}$$

$$s(t, t_1, t_2, q_1, \boldsymbol{\omega_1}, q_2, \boldsymbol{\omega_2}, f) = f \arccos D_s, \tag{31}$$

$$E_s(t,t_1,t_2,q_1,\boldsymbol{\omega_1},q_2,\boldsymbol{\omega_2},f) = scalar\ part\{E\} \in R , \tag{32}$$

$$\mathbf{E_v}(t,t_1,t_2,q_1,\boldsymbol{\omega_1},q_2,\boldsymbol{\omega_2},f) = vector\ part\{E\} \in R^3 , \tag{33}$$

$$E_s(t,t_1,t_2,q_1,\boldsymbol{\omega_1},q_2,\boldsymbol{\omega_2},f) = \cos s , \tag{34}$$

$$\mathbf{E_v}(t,t_1,t_2,q_1,\boldsymbol{\omega_1},q_2,\boldsymbol{\omega_2},f) = \hat{\mathbf{D}}_v \sin s , \tag{35}$$

$$q(t,t_1,t_2,q_1,\boldsymbol{\omega_1},q_2,\boldsymbol{\omega_2},f) = E \otimes C_1 . \tag{36}$$

A straightforward differentiation of the equations above with respect to time t leads to the following formula for the angular velocity:

$$\dot{C}_1(t,t_1,q_1,\boldsymbol{\omega_1}) = -\frac{\|\boldsymbol{\omega_1}\|}{2}\sin\left[\frac{\|\boldsymbol{\omega_1}\|}{2}(t-t_1)\right]q_1 + \cos\left[\frac{\|\boldsymbol{\omega_1}\|}{2}(t-t_1)\right]\dot{q}_1 , \tag{37}$$

$$\dot{C}_2(t,t_2,q_2,\boldsymbol{\omega_2}) = -\frac{\|\boldsymbol{\omega_2}\|}{2}\sin\left[\frac{\|\boldsymbol{\omega_2}\|}{2}(t-t_2)\right]q_2 + \cos\left[\frac{\|\boldsymbol{\omega_2}\|}{2}(t-t_2)\right]\dot{q}_2 , \tag{38}$$

$$\dot{D}(t,t_1,t_2,q_1,\boldsymbol{\omega_1},q_2,\boldsymbol{\omega_2}) = \dot{C}_2 \otimes \overline{C}_1 + \dot{C}_2 \otimes \overline{\dot{C}}_1 , \tag{39}$$

$$\dot{s}(t,t_1,t_2,q_1,\boldsymbol{\omega_1},q_2,\boldsymbol{\omega_2},f) = \dot{f}\arccos D_s - f\frac{\dot{D}_s}{D_v} , \tag{40}$$

$$\dot{E}_s(t,t_1,t_2,q_1,\boldsymbol{\omega_1},q_2,\boldsymbol{\omega_2},f) = -\dot{s}\sin s , \tag{41}$$

$$\dot{\mathbf{E}}_v(t,t_1,t_2,q_1,\boldsymbol{\omega_1},q_2,\boldsymbol{\omega_2},f) = \hat{\mathbf{D}}_v\dot{s}\cos s + \hat{\mathbf{D}}_v\frac{D_s\dot{D}_s\sin s}{D_v^2} + \dot{\mathbf{D}}_v\frac{\sin s}{D_v} , \tag{42}$$

$$\dot{q}(t,t_1,t_2,q_1,\boldsymbol{\omega_1},q_2,\boldsymbol{\omega_2},f) = \dot{E} \otimes C_1 + E \otimes \dot{C}_1 , \tag{43}$$

$$\boldsymbol{\omega}(t,t_1,t_2,q_1,\boldsymbol{\omega_1},q_2,\boldsymbol{\omega_2},f) = 2 \times vector\ part\{\dot{q} \otimes \overline{q}\} . \tag{44}$$

Then, another differentiation leads to the following formula for the angular acceleration:

$$\ddot{C}_1(t,t_1,q_1,\boldsymbol{\omega_1}) = -\frac{\|\boldsymbol{\omega_1}\|^2}{4}C_1 , \tag{45}$$

$$\ddot{C}_2(t,t_2,q_2,\boldsymbol{\omega_2}) = -\frac{\|\boldsymbol{\omega_2}\|^2}{4}C_2 , \tag{46}$$

$$\ddot{D}(t,t_1,t_2,q_1,\boldsymbol{\omega_1},q_2,\boldsymbol{\omega_2}) = -\frac{1}{4}\left(\|\boldsymbol{\omega}_1\|^2 + \|\boldsymbol{\omega}_2\|^2\right)D + 2\dot{C}_2 \otimes \overline{\dot{C}}_1, \tag{47}$$

$$\ddot{s}(t,t_1,t_2,q_1,\boldsymbol{\omega_1},q_2,\boldsymbol{\omega_2},f) = \ddot{f}\arccos D_s - 2\dot{f}\frac{\dot{D}_s}{D_v} - f\left(\frac{\ddot{D}_s}{D_v} + \frac{D_s\dot{D}_s^2}{D_v^3}\right), \tag{48}$$

$$\ddot{E}_s(t,t_1,t_2,q_1,\boldsymbol{\omega_1},q_2,\boldsymbol{\omega_2},f) = -\dot{s}^2 E_s - \ddot{s}\sin s, \tag{49}$$

$$\begin{aligned}
\ddot{\mathbf{E}}_\mathbf{v}(t,t_1,t_2,q_1,\boldsymbol{\omega_1},q_2,\boldsymbol{\omega_2},f) &= -\mathbf{E}_\mathbf{v}\dot{s}^2 \\
&+ \hat{\mathbf{D}}_\mathbf{v}\left[\ddot{s}\cos s + 3\frac{D_s^2\dot{D}_s^2\sin s}{D_v^4} + \frac{2\dot{s}D_s\dot{D}_s\cos s + \dot{D}_s^2\sin s + D_s\ddot{D}_s\sin s}{D_v^2}\right], \\
&+ 2\dot{\mathbf{D}}_\mathbf{v}\left[\frac{\dot{s}\cos s}{D_v} + \frac{D_s\dot{D}_s\sin s}{D_v^3}\right] + \ddot{\mathbf{D}}_\mathbf{v}\frac{\sin s}{D_v}
\end{aligned} \tag{50}$$

$$\ddot{q}(t,t_1,t_2,q_1,\boldsymbol{\omega_1},q_2,\boldsymbol{\omega_2},f) = \ddot{E} \otimes C_1 + E \otimes \ddot{C}_1 + 2\dot{E} \otimes \dot{C}_1, \tag{51}$$

$$\dot{\boldsymbol{\omega}}(t,t_1,t_2,q_1,\boldsymbol{\omega_1},q_2,\boldsymbol{\omega_2},f) = 2 \times vector\ part\{\ddot{q} \otimes \overline{q}\}. \tag{52}$$

Linearized expressions for the angular velocity and acceleration can be presented as a linear combination of the following basis vectors and basis coordinates:

$$q_d(q_1,q_2) = q_2 \otimes \overline{q}_1, \tag{53}$$

$$\mathbf{Q_1}(q_1,\boldsymbol{\omega_1},q_2,\boldsymbol{\omega_2}) = 2 \times vector\ part\{q_d\}, \tag{54}$$

$$\mathbf{Q_2}(q_1,\boldsymbol{\omega_1},q_2,\boldsymbol{\omega_2}) = 2 \times vector\ part\{\dot{q}_1 \otimes \overline{q}_1\} = \boldsymbol{\omega}_1, \tag{55}$$

$$\mathbf{Q_3}(q_1,\boldsymbol{\omega_1},q_2,\boldsymbol{\omega_2}) = 2 \times vector\ part\{\dot{q}_2 \otimes \overline{q}_1\} = vector\ part\{\boldsymbol{\omega}_2 \otimes q_d\}, \tag{56}$$

$$\mathbf{Q_4}(q_1,\boldsymbol{\omega_1},q_2,\boldsymbol{\omega_2}) = 2 \times vector\ part\{\dot{q}_1 \otimes \overline{q}_2\} = vector\ part\{\boldsymbol{\omega}_1 \otimes \overline{q}_d\}, \tag{57}$$

$$\mathbf{Q_5}(q_1,\boldsymbol{\omega_1},q_2,\boldsymbol{\omega_2}) = 2 \times vector\ part\{\dot{q}_2 \otimes \overline{q}_2\} = \boldsymbol{\omega}_2, \tag{58}$$

$$\begin{aligned}
\mathbf{Q_6}(q_1,\boldsymbol{\omega_1},q_2,\boldsymbol{\omega_2}) &= 2 \times vector\ part\{\dot{q}_2 \otimes \overline{\dot{q}}_1\} \\
&= -vector\ part\{\boldsymbol{\omega}_2 \otimes q_d \otimes \boldsymbol{\omega}_1\}/2,
\end{aligned} \tag{59}$$

$$T = t_2 - t_1, \tag{60}$$

$$F_1(f,t,t_1,t_2) = \dot{f}, \tag{61}$$

$$F_2(f,t,t_1,t_2) = (1-f)^2/T, \tag{62}$$

$$F_3(f,t,t_1,t_2) = \left[f(1-f) + \dot{f}(t-t_2)\right]/T , \tag{63}$$

$$F_4(f,t,t_1,t_2) = \left[f(1-f) - \dot{f}(t-t_1)\right]/T , \tag{64}$$

$$F_5(f,t,t_1,t_2) = f^2/T , \tag{65}$$

$$F_6(f,t,t_1,t_2) = \dot{f}(t-t_1)(t-t_2)/T^2 + (1-f)f/T , \tag{66}$$

$$\dot{F}_1(f,t,t_1,t_2) = \ddot{f} , \tag{67}$$

$$\dot{F}_2(f,t,t_1,t_2) = -2\dot{f}(1-f)/T , \tag{68}$$

$$\dot{F}_3(f,t,t_1,t_2) = \left[\ddot{f}(t-t_2) + 2\dot{f}(1-f)\right]/T , \tag{69}$$

$$\dot{F}_4(f,t,t_1,t_2) = -\left[2\dot{f}f + \ddot{f}(t-t_1)\right]/T , \tag{70}$$

$$\dot{F}_5(f,t,t_1,t_2) = 2\dot{f}f/T , \tag{71}$$

$$\dot{F}_6(f,t,t_1,t_2) = \left[\ddot{f}(t-t_1)(t-t_2) + 2\dot{f}(t-t_2 f - t_1(1-f))\right]/T^2 . \tag{72}$$

Finding optimal quartic blending function requires solving for the optimal quartic parameter, which is the root of a cubic polynomial with the following coefficients:

$$a_0(t_1,t_2,q_1,\boldsymbol{\omega_1},q_2,\boldsymbol{\omega_2}) =$$

$$\frac{2T}{105}\left[-168W_{13} + 168W_{14} + 4W_{22} + 3W_{23} - 11W_{24} + 2W_{25}\right]$$

$$+ \frac{2T}{105}\left[77W_{33} + 11W_{35} + 5W_{36} - 77W_{44} - 3W_{46} - 4W_{55} - 2W_{56}\right] \tag{73}$$

$$a_1(t_1,t_2,q_1,\boldsymbol{\omega_1},q_2,\boldsymbol{\omega_2}) =$$

$$\frac{T^5}{45045}\left[18018W_{11} - 2574W_{12} - 15444W_{13} - 15444W_{14} - 2574W_{15} - 2574W_{16}\right]$$

$$+ \frac{T^5}{45045}\left[500W_{22} + 716W_{23} + 1574W_{24} - 716W_{25} + 352W_{26}\right]$$

$$+ \frac{T^5}{45045}\left[5648W_{33} + 1858W_{34} + 1574W_{35} + 935W_{36}\right] \tag{74}$$

$$+ \frac{T^5}{45045}\left[5648W_{44} + 716W_{45} + 935W_{46} + 500W_{55} + 352W_{56} + 149W_{66}\right]$$

$$a_2(t_1, t_2, q_1, \boldsymbol{\omega_1}, q_2, \boldsymbol{\omega_2}) =$$

$$-\frac{T^9}{2310}\left[4W_{22} - 9W_{23} + W_{24} - 4W_{25} + 5W_{33} - W_{35}\right] \quad , \tag{75}$$

$$-\frac{T^9}{2310}\left[5W_{36} - 5W_{44} + 9W_{45} - 5W_{46} - 4W_{55} + 4W_{56}\right]$$

$$a_3(t_1, t_2, q_1, \boldsymbol{\omega_1}, q_2, \boldsymbol{\omega_2}) =$$

$$\frac{4T^{13}}{45045}\left[W_{22} - 2W_{23} - 2W_{24} + 2W_{25} - 2W_{26} + W_{33} + 2W_{34} - 2W_{35}\right]. \tag{76}$$

$$+\frac{4T^{13}}{45045}\left[2W_{36} + W_{44} - 2W_{45} + 5W_{46} + W_{55} - 2W_{56} + W_{66}\right]$$